Supplementary Information

Charge-transfer dynamics at the dye-semiconductor interface of photocathodes for solar energy applications

Fiona A. Black[a], Christopher J. Wood[b], Simbarashe Ngwerume[b], Gareth H. Summers[a], Ian P. Clark[d], Michael Towrie[d], Jason E. Camp*[b,c], Elizabeth A. Gibson*[a,b].

[a] *School of Chemistry, Newcastle University, Newcastle upon Tyne, NE1 7RU, UK*

[b] *School of Chemistry, The University of Nottingham, University Park, Nottingham, NG7 2RD, UK.*

[c] *Department of Chemical Sciences, University of Huddersfield, Queensgate, Huddersfield, HD1 3DH, UK.*

[d] *Central Laser Facility, Research Complex at Harwell, Science and Technology Facilities Council, Rutherford Appleton Laboratory, Harwell Campus, Didcot, Oxfordshire, OX11 0QX, United Kingdom*

^{1}H, ^{13}C NMR and 2D NMR spectra of CAD4

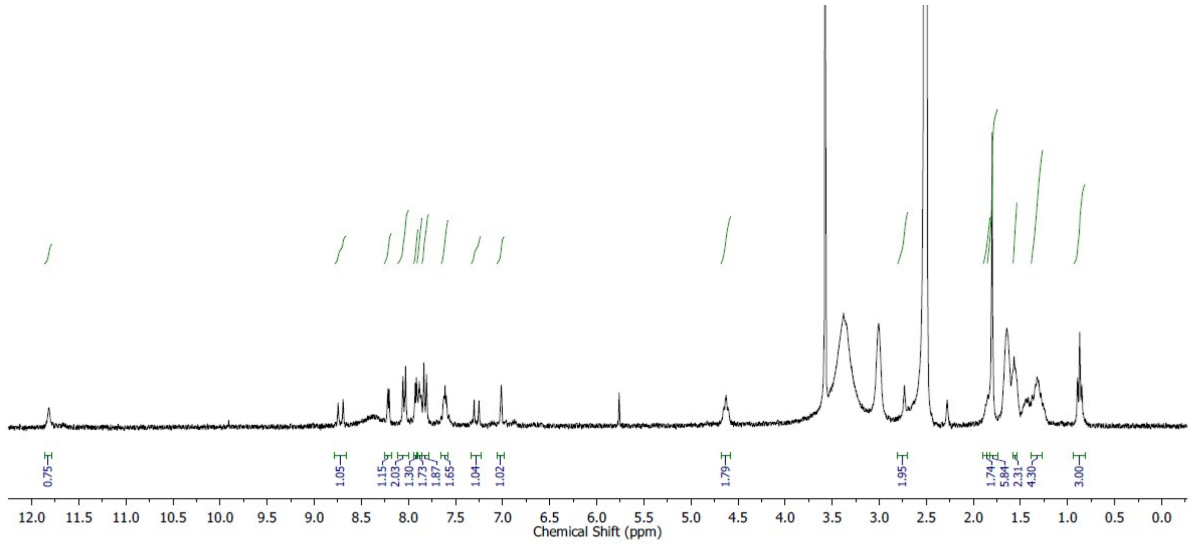

Figure S 1 ^{1}H NMR spectrum of CAD4 (DMSO, 300 MHz).

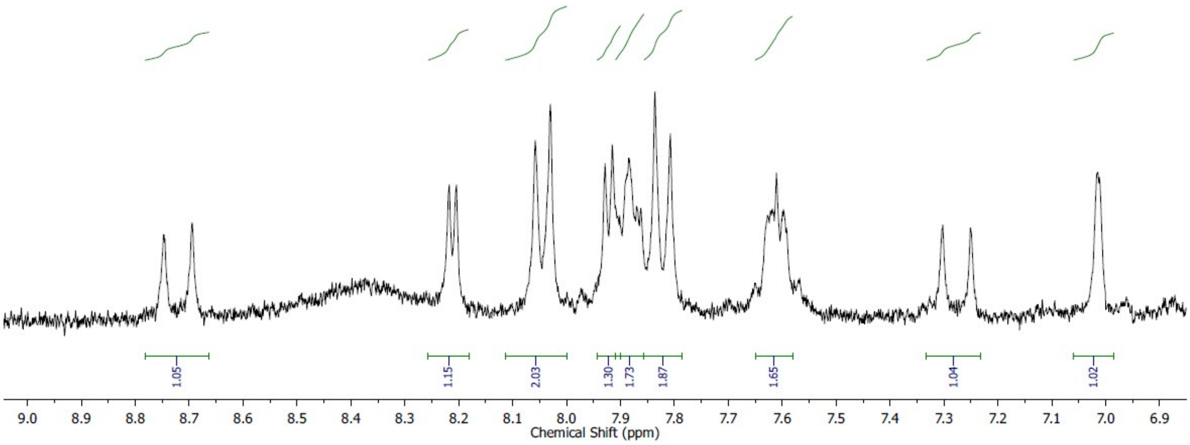

Figure S 2 ^{1}H NMR spectrum of CAD4 (DMSO, 300 MHz), expansion of the aromatic region.

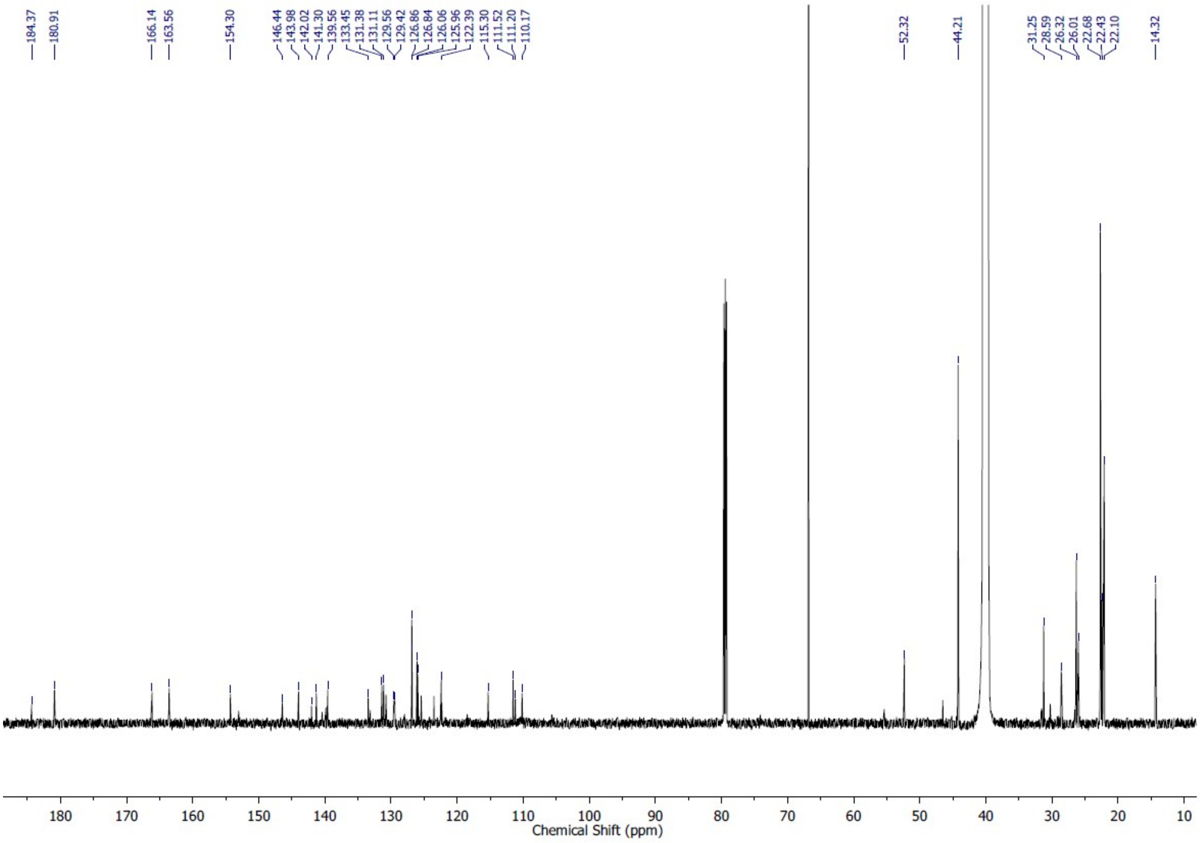

Figure S 3 ^{13}C NMR spectrum of CAD4 (DMSO, 700 MHz).

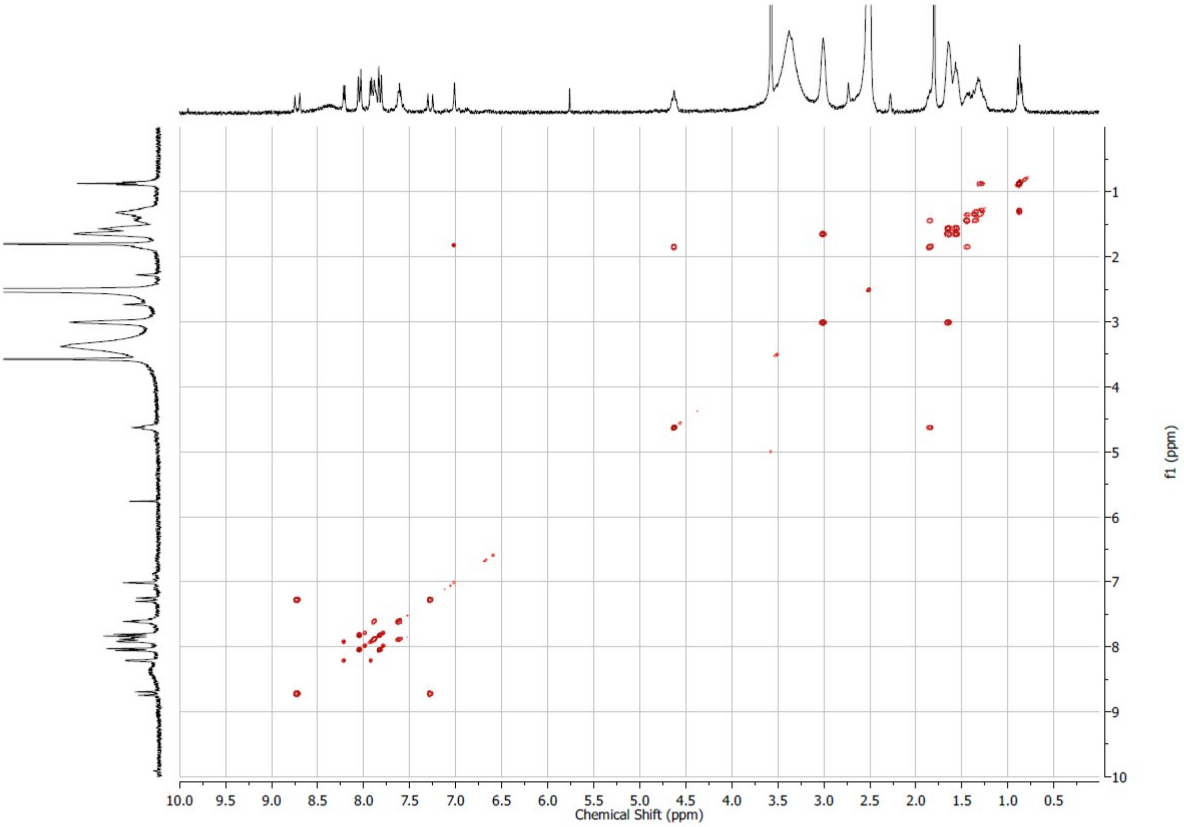

Figure S 4 COSY NMR spectrum of CAD4 (DMSO, 700 MHz).

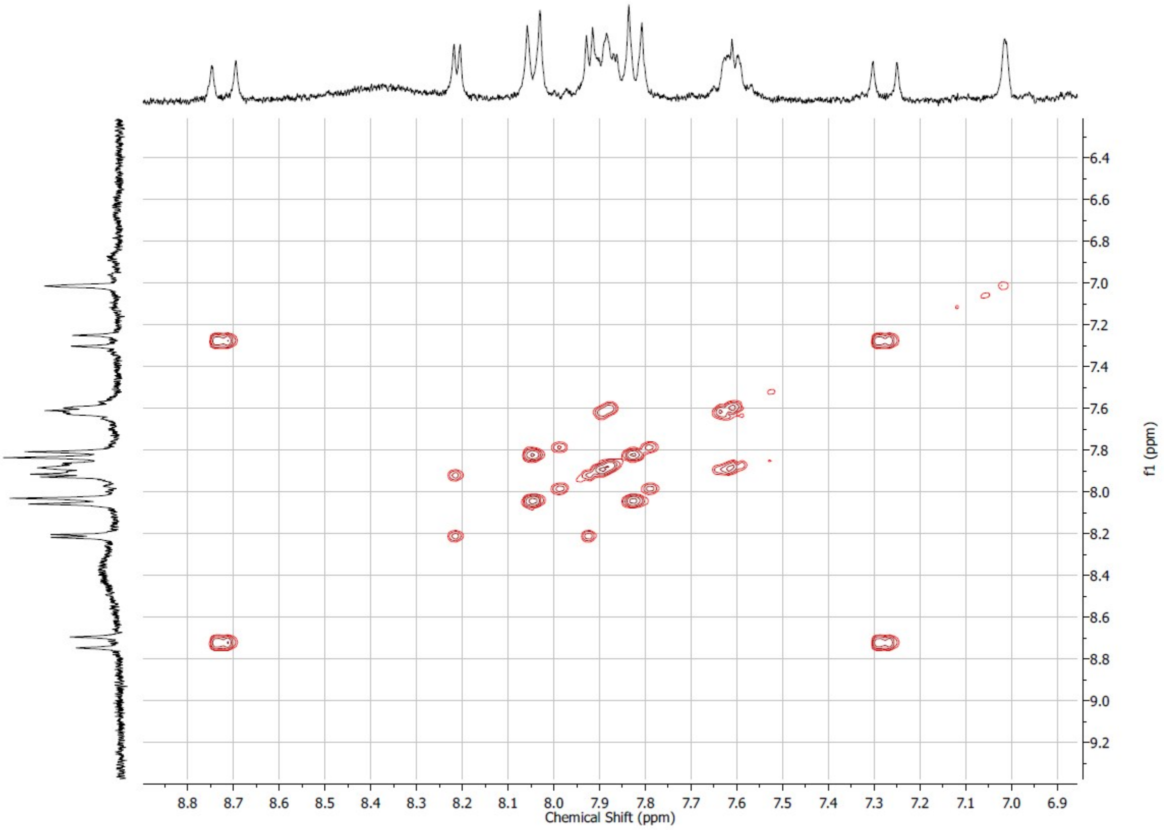

Figure S 5 COSY NMR spectrum of CAD4 (DMSO, 700 MHz), expansion of the aromatic region.

UV-visible absorption and emission spectra of CAD3 and CAD4

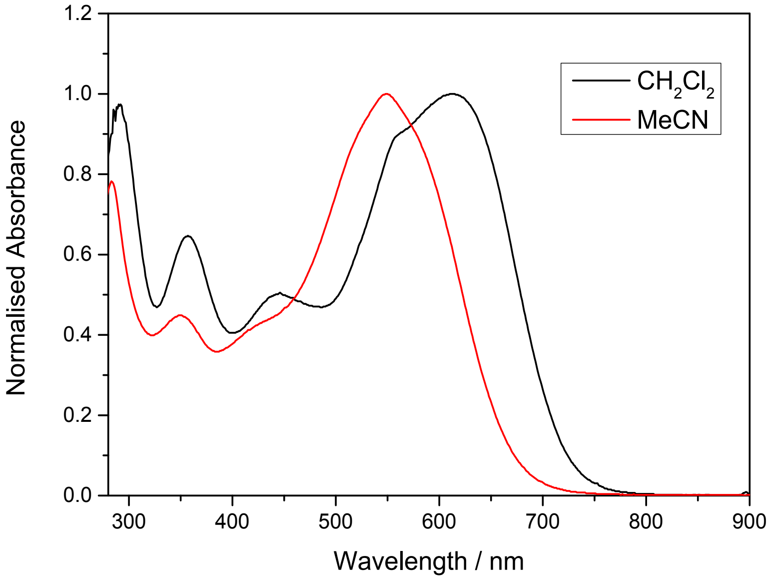

Figure S 6 Normalised absorption spectra of CAD3 dissolved in CH_2Cl_2 (black line) and MeCN (red line).

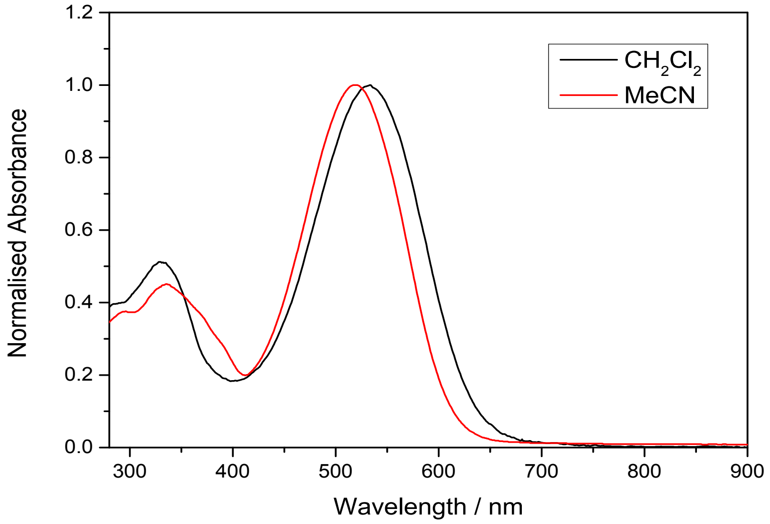

Figure S 7 Normalised absorption spectra of CAD4 dissolved in CH_2Cl_2 (black line) and MeCN (red line).

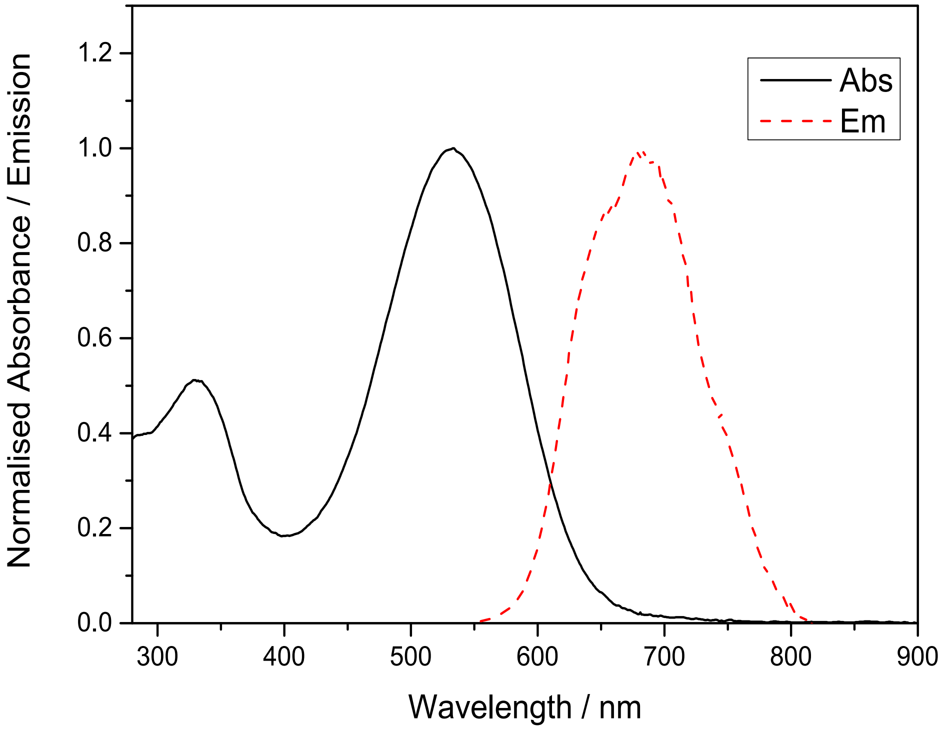

Figure S 8 Normalised absorbance and emission spectra of CAD4 inCH_2Cl_2

Infrared spectra of CAD3, CAD4 and their precursors

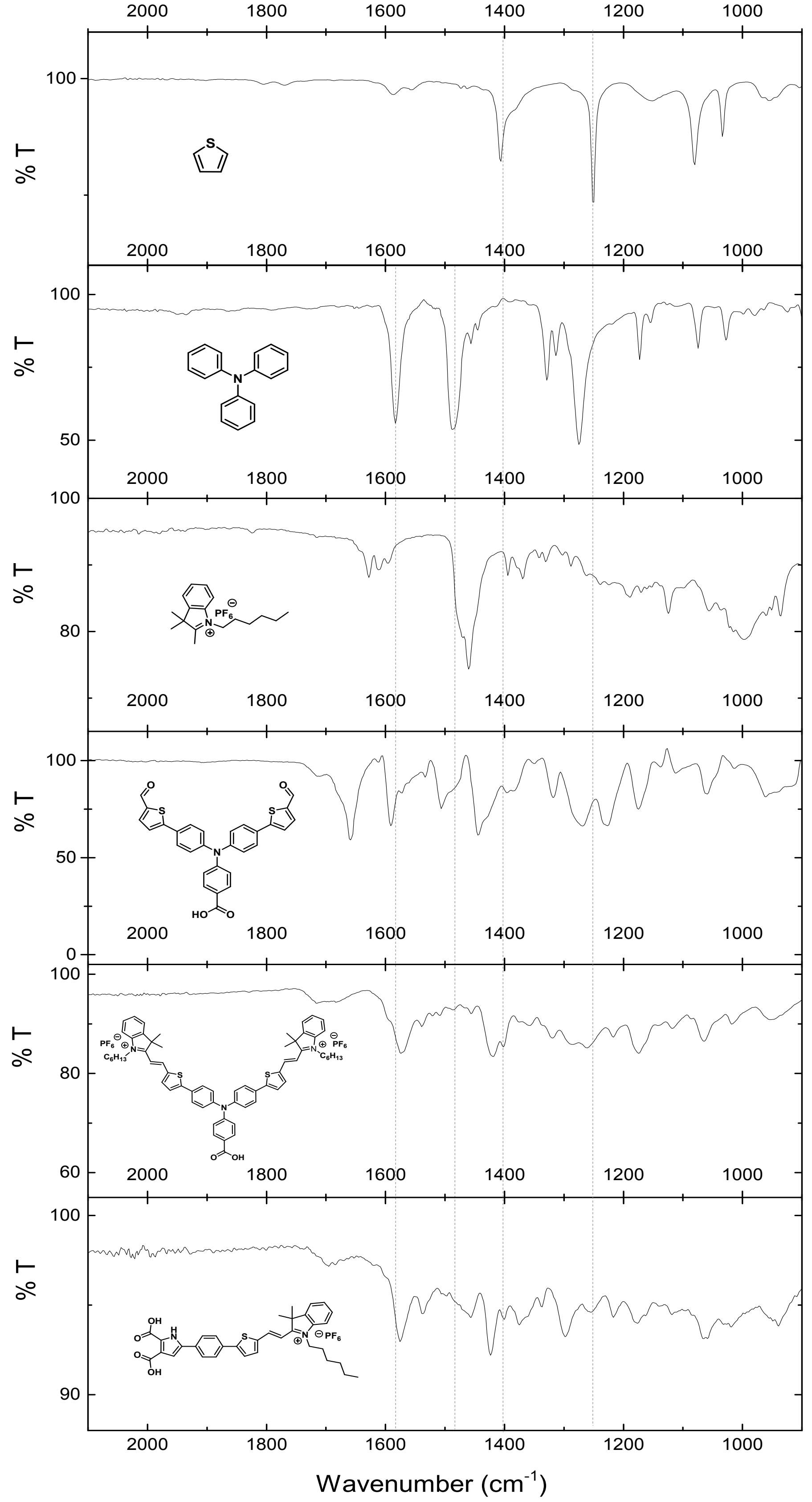

Figure S 9 Ground state infrared spectra of CAD3 and CAD4 and their precursors. All spectra were run on solid samples using attenuated total reflectance (ATR).

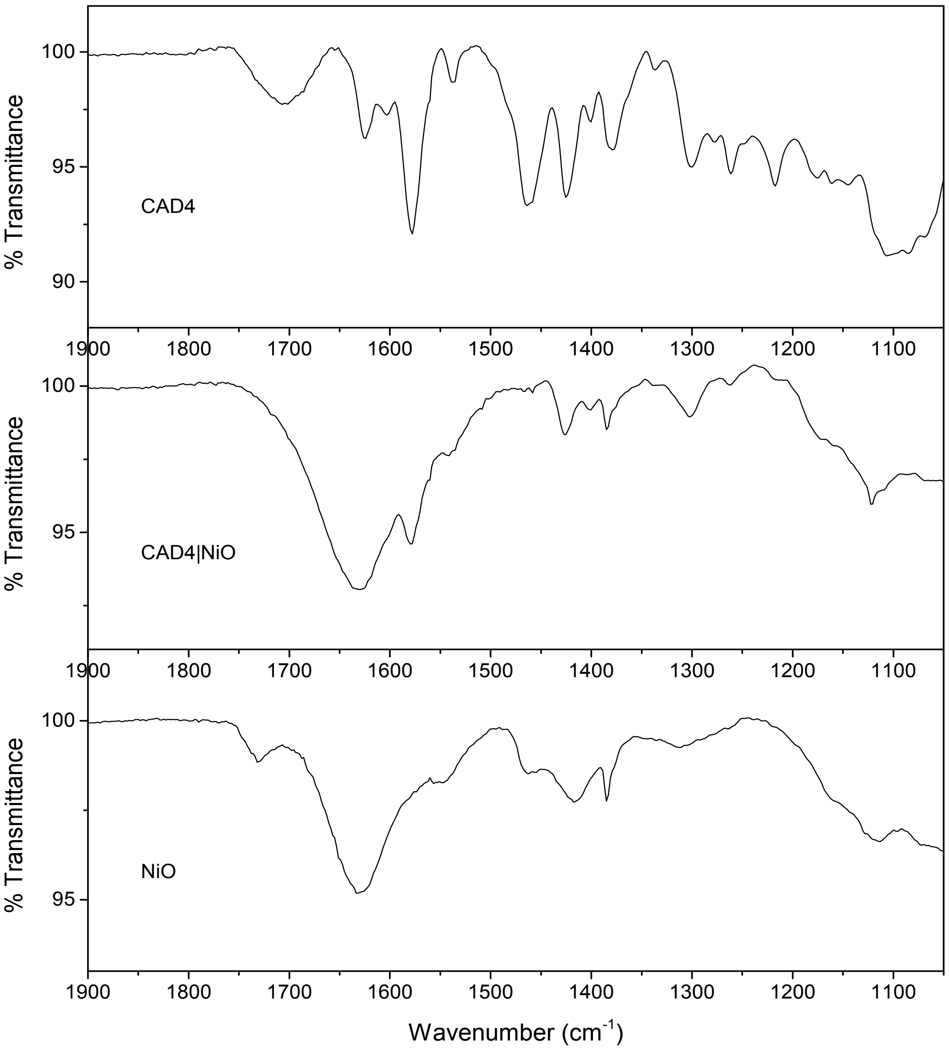

Figure S 10 Ground state FT-IR spectra of CAD4 as a solid (top), adsorbed on NiO (middle) and undyed NiO (bottom). All samples were measured as solids in KBr discs.

Molecular modelling

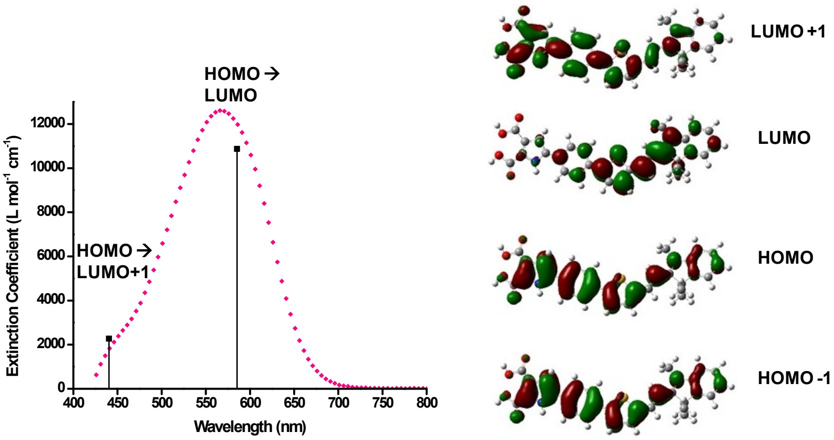

Figure S 11 The absorption spectra of CAD4 in dichloromethane. The calculated electronic transitions have been overlaid for comparison. The isodensity plots of the orbitals involved in these transitions are shown to the right. These isodensity plots show significant overlap in electron density between the HOMO and LUMO.

The calculated electronic transitions and corresponding orbitals for CAD4 are summarised in Table S 1. From the isodensity plots a shift in electron density from anchor donor unit to the cationic acceptor corresponding to the HOMO → LUMO transition is observed. The LUMO of the dye extends throughout the molecule with the exception of the pyrrole-2,3-dicaboxylic acid. The two carboxylic acids on the pyrrole donor have substantial electron withdrawing properties. The shift of electron density away from these demonstrates the strong electron withdrawing nature of the cationic indolium and should facilitate charge transfer away from the NiO surface and towards the electrolyte. B3LYP is known to underestimate the energy of 'charge transfer like' electronic transitions.[1,2] The error observed between the λ_{max} predicted by TDDFT and the λ_{max} determined experimentally is much smaller for CAD4 (+ 19 nm) than those for CAD1-3 (73-115 nm).

Dye	Molecular Orbital	Energy (eV)
CAD4	LUMO +1	-1.96
	LUMO	-3.60
	HOMO	-5.93
	HOMO -1	-6.64

Table S 1 The calculated electronic transitions for CAD4.

Electrochemical studies

Cyclic voltammetry and differential pulse voltammetry (DPV) were carried out using an IVIUM Compactstat potentiostat. The experiments were carried out under an atmosphere of argon using a three-electrode arrangement in a single compartment cell. A glassy carbon working electrode, a Pt wire secondary electrode and a Ag/AgNO$_3$ (0.01 M AgNO$_3$ in CH$_2$Cl$_2$) reference electrode, were used in the cell. The CH$_2$Cl$_2$ solutions were 10^{-3} M in test compound and 0.5 M in [NBu$_4$][ClO$_4$] as supporting electrolyte. Redox potentials are quoted versus the ferrocenium-ferrocene couple used as an external reference. Compensation for internal resistance was not applied.

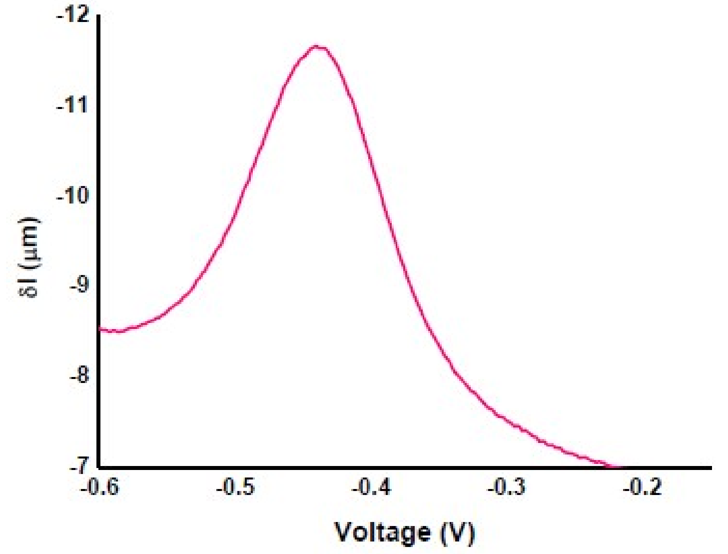

Figure S 12 Differential pulse voltammogram of CAD4.

Solar cell measurements

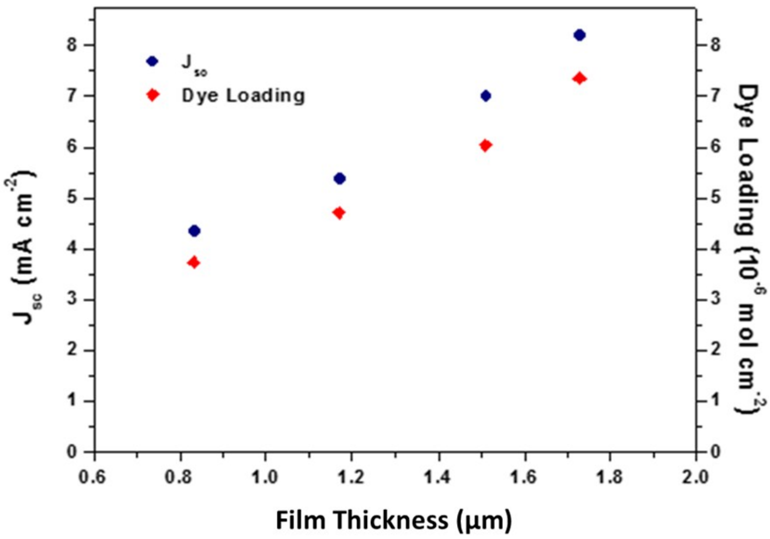

Figure S 13 Jsc/dye loading vs. film thickness of p-DSCs sensitised with CAD3.

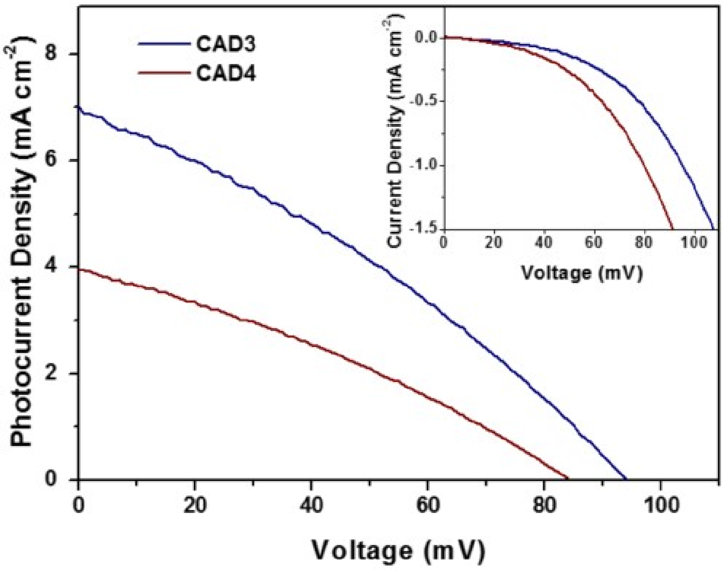

Figure S 14 Photocurrent density vs. voltage curves and dark current (inset) curves for p-DSCs sensitised by CAD3 (blue line) and CAD4 (red line).

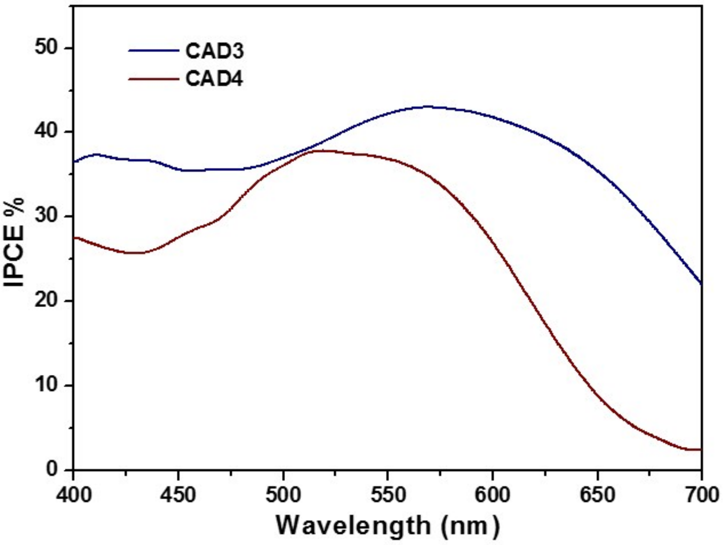

Figure S 15 IPCE spectra for p-DSCs sensitised by CAD3 (blue line) and CAD4 (red line).

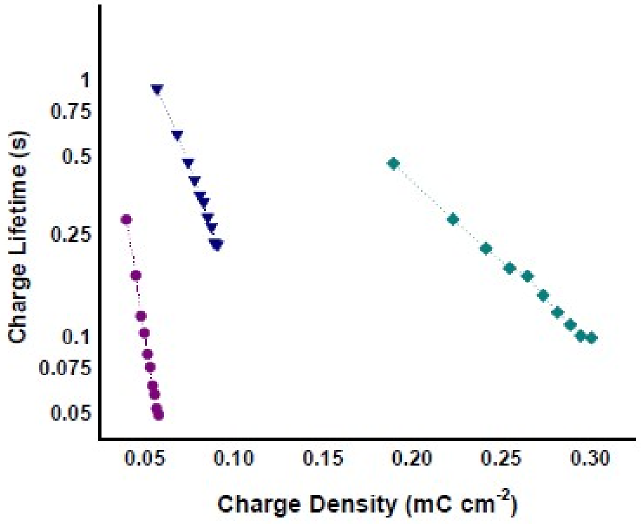

Figure S 16 Charge lifetime vs. extracted charge density plots for p-DSCs sensitised with CAD1 (purple), CAD2 (blue) and CAD3 (cyan).

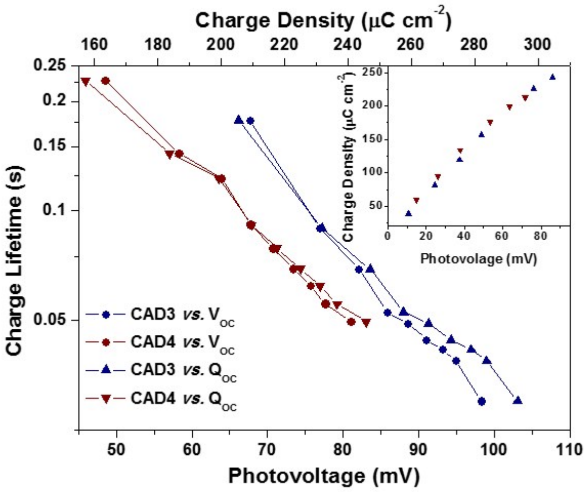

Figure S 17 Charge lifetime vs. photovoltage/extracted charge density and extracted charge density vs. photovoltage (inset) plots for p-DSCs sensitised with CAD3 (blue) and CAD4 (red).

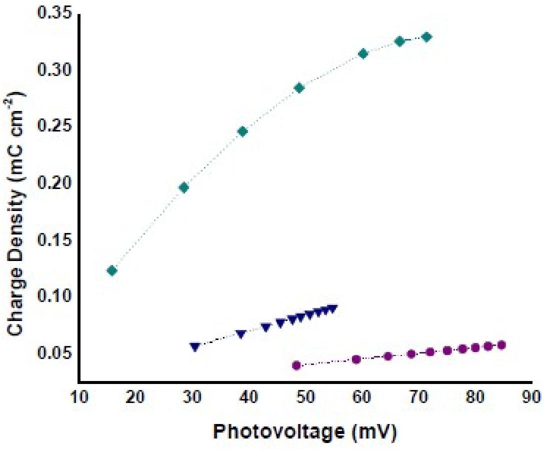

Figure S 18 Extracted charge density vs. photovoltage for p-DSCs sensitised with CAD1 (purple), CAD2 (blue) and CAD3 (cyan).

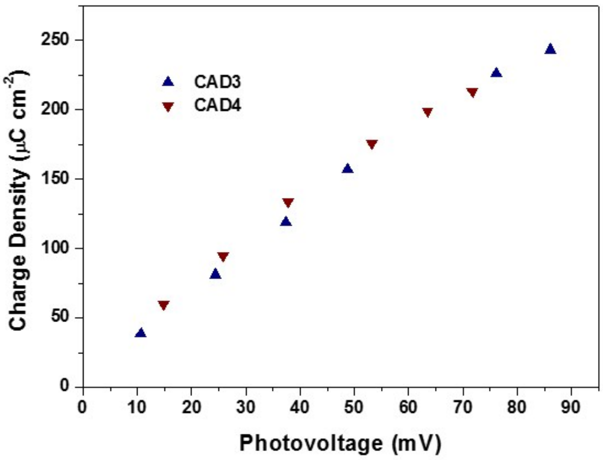

Figure S 19 Extracted charge density vs. photovoltage plot for CAD3 (blue) and CAD4 (red).

Spectroelectrochemistry

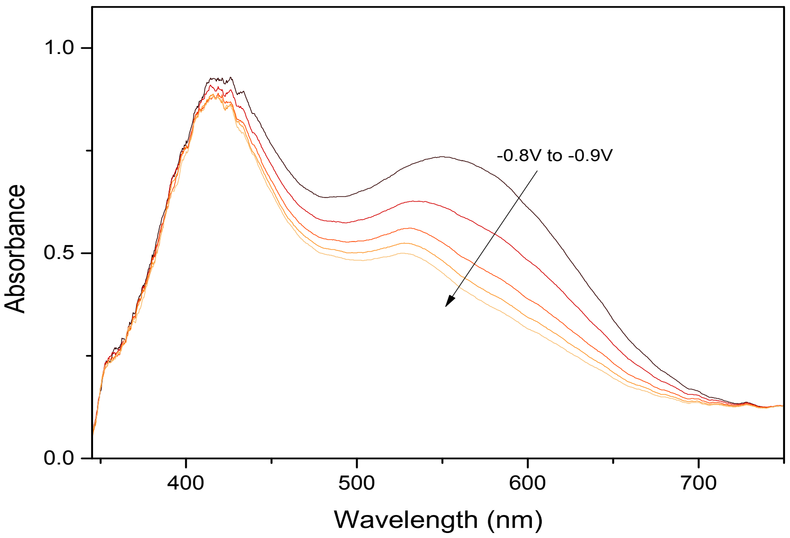

Figure S 20 UV-Visible spectrum of CAD3 immobilised on TiO_2/FTO working electrode upon reduction, with 0.1M $TBAClO_4$ supporting electrolyte, a platinum counter electrode and a $Ag/AgNO_3$ reference electrode.

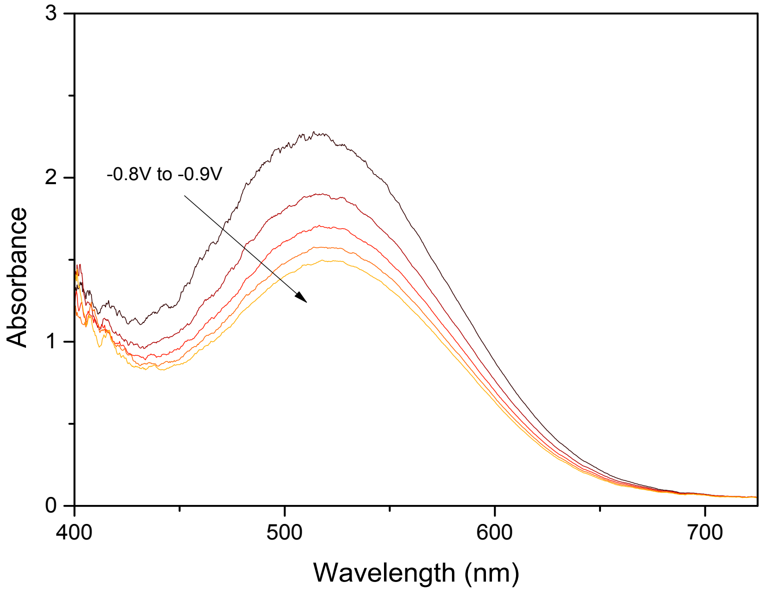

Figure S 21 UV-Visible spectrum of CAD4 immobilised on TiO_2/FTO working electrode upon reduction, with 0.1M $TBAClO_4$ supporting electrolyte, a platinum counter electrode and a $Ag/AgNO_3$ reference electrode.

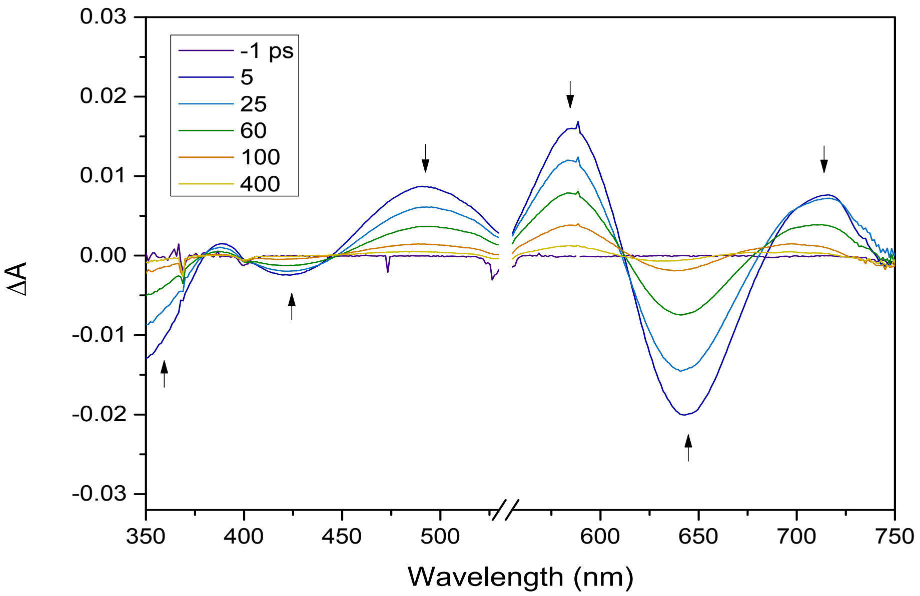

Figure S 22 Transient absorption spectrum of CAD3 in CH_2Cl_2, at various delay times after excitation at 532 nm.

Wavelength (nm)	Peak	τ_1 (ps)
354	Bleach	52 ± 2
387	Peak	57 ± 3
425	Bleach	73 ± 2
485	Peak	55 ± 4
575	Peak	90 ± 7
635	Bleach	48 ± 1
701	Peak	63 ± 3
Average lifetime τ = 63 ± 3		

Table S 2 Kinetic data from transient absorption measurements for CAD3 in CH_2Cl_2.

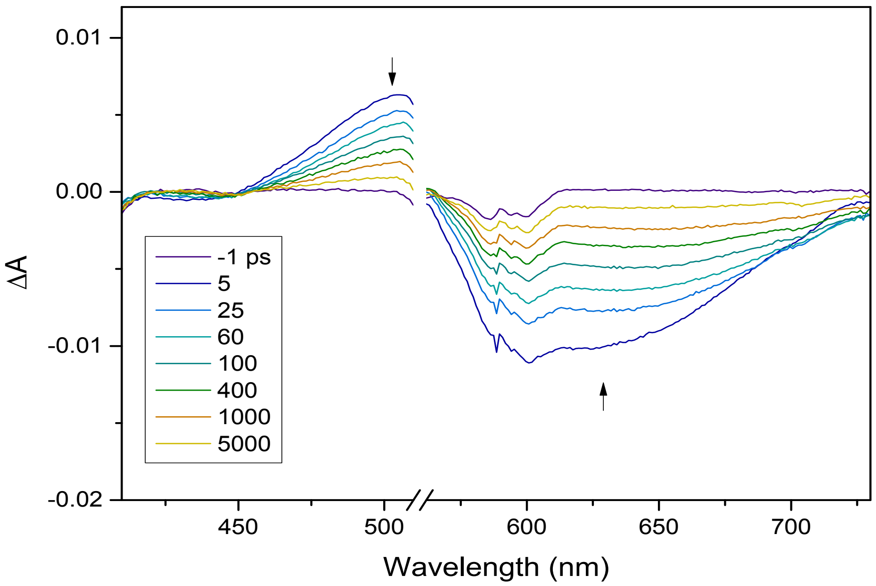

Figure S 23 Transient absorption spectra for CAD3|NiO at various delay times after excitation at 532 nm.

Wavelength (nm)	Peak	τ_1 (ps)	A_1	τ_2 (ps)	A_2	τ_3 (ns)	A_3	y_0 (%)	Weighted average (ns)
428	Bleach	7 ± 3	55 %	268 ± 94	45 %			0	0.12
485	Peak	5 ± 1	37 %	120 ± 25	34 %	4.5 ± 1.0	26 %	3	1.21
610	Bleach	12 ± 2	38 %	181 ± 33	40 %	7.3 ± 1.6	22 %	4	1.68

Table S 3 Kinetic data from transient absorption measurements for CAD3|NiO. The amplitude weighted average lifetime here is based on τ for comparison with the amplitude weighted lifetime based on logτ provided in the main text.

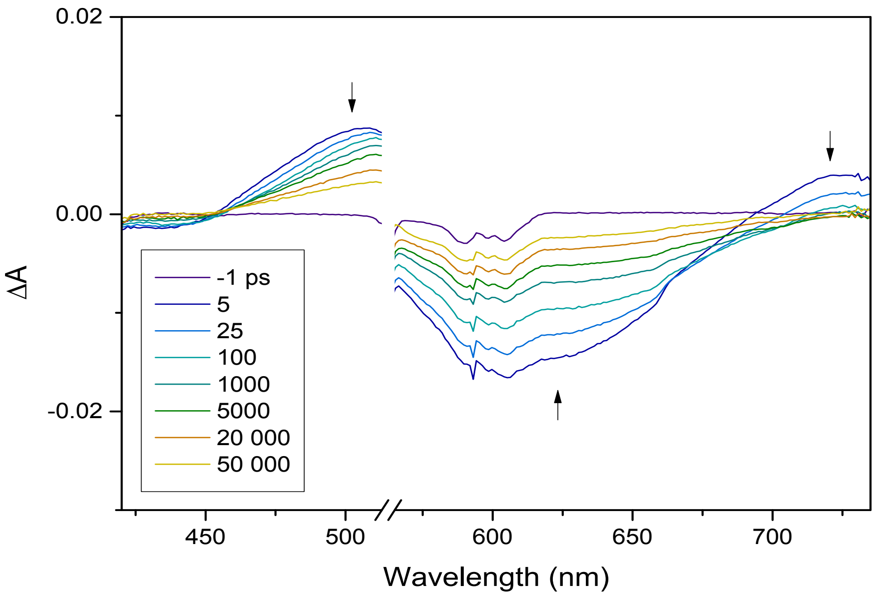

Figure S 24 Transient absorption spectrum for CAD3|NiO in the presence of I^-/I_3^-, taken at various delay times after excitation at 532 nm.

.

Wavelength (nm)	Peak	τ_1 (ps)	A_1	τ_2 (ns)	A_2	τ_3 (ns)	A_3	y_0 (%)	Weighted average (ns)
435	Bleach	150 ± 50	42%	22 ± 6	58%			0	12.8
485	Peak	24 ± 4	30%	9.1 ± 1.8	35%	311 ± 84	29%	6	93.3
615	Bleach	18 ± 3	32%	0.76 ± 0.13	34%	54 ± 10	28%	7	15.4
720	Peak	16 ± 7							0.016

Table S 4 Kinetic data from transient absorption measurements of CAD3|NiO|I^-/I_3^-. The amplitude weighted average lifetime here is based on τ for comparison with the amplitude weighted lifetime based on logτ provided in the main text.

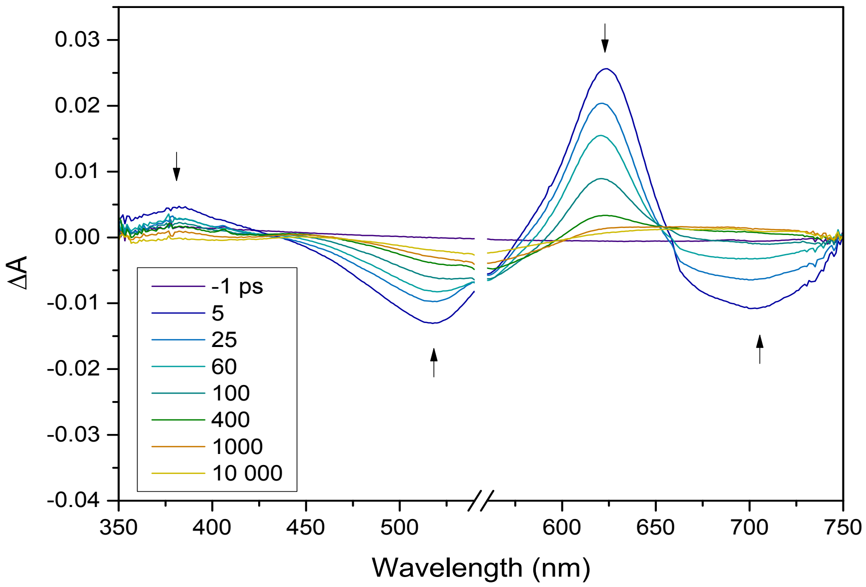

Figure S 25 Transient absorption spectra of CAD4 in CH_2Cl_2 solution at various delay times after excitation at 532 nm.

Wavelength (nm)	Peak	τ_1 (ps)	A_1	τ_2 (ps)	A_2	y_0 (%)	Weighted average (ps)
389	Peak	4 ± 0.4	39 %	253 ± 55	44 %	17	113
518	Bleach	9 ± 2	35 %	195 ± 24	50 %	15	101
627	Peak	43 ± 8	50 %	240 ± 50	47 %	3	134
702	Bleach	5 ± 3	32 %	59 ± 10	68 %	0	42

Table S 5 Kinetic data from transient absorption measurements of CAD4 in CH_2Cl_2. The amplitude weighted average lifetime here is based on τ for comparison with the amplitude weighted lifetime based on logτ provided in the main text.

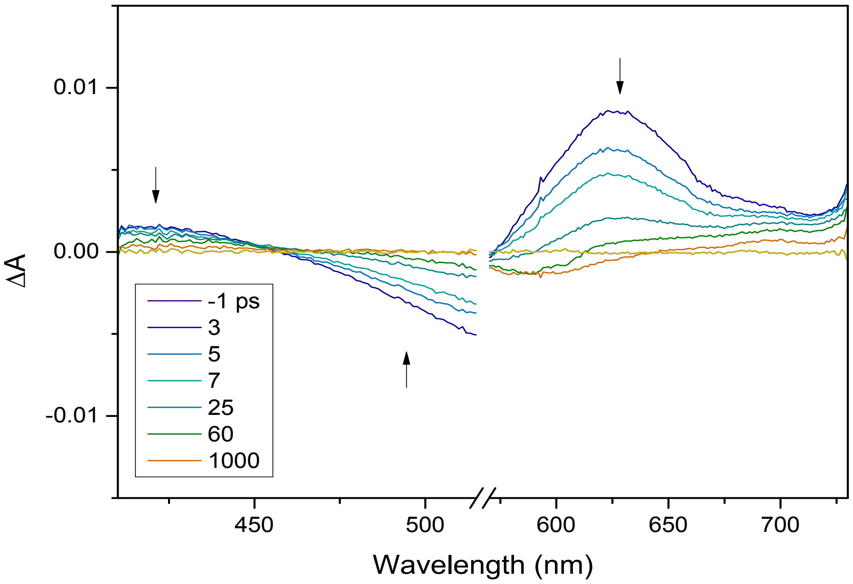

Figure S 26 Transient absorption data for CAD4|NiO at various delay times after excitation at 532 nm.

Wavelength (nm)	Peak	τ_1 (ps)	A_1	τ_2 (ps)	A_2	y_0 (%)	Weighted average (ps)
500	Bleach	3 ± 0.3	73 %	43 ± 6	27 %	0	14
640	Peak	2 ± 0.1	79 %	35 ± 6	21 %	0	9
Overall weighted average, τ = 12 ps							

Table S 6 Kinetic data from transient absorption measurements for CAD4|NiO. The amplitude weighted average lifetime here is based on τ for comparison with the amplitude weighted lifetime based on logτ provided in the main text.

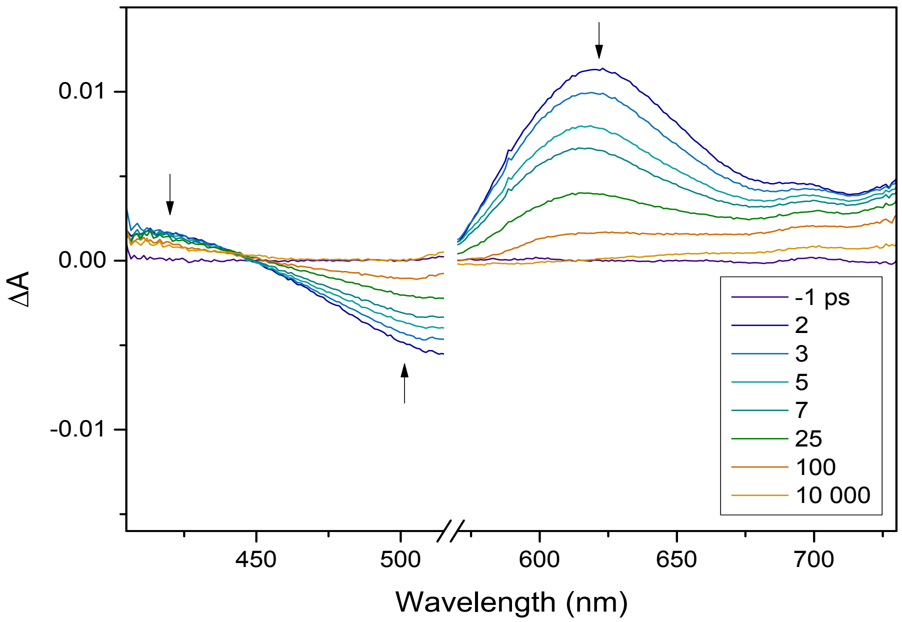

Figure S 27 Transient absorption spectrum for CAD4|NiO in the presence of I^-/I_3^-, taken at various delay times after excitation at 532 nm.

Wavelength (nm)	Peak	τ_1 (ps)	A_1	τ_2 (ps)	A_2	τ_3 (ns)	A_3	y_0 (%)	Weighted average (ps)
495	Bleach	3 ± 0.1	59%	33 ± 9	25%	1.4 ± 0.4	18%	0	262
625	Peak	3 ± 0.1	64%	28 ± 4	25%	0.74 ± 0.18	11%	0	90
696	Peak	0.8 ± 0.3	66%	20 ± 8	15%	1.0 ± 0.4	14%	5	143
704	Peak	3 ± 1	45%	105 ± 47	26%	6.1 ± 3.1	20%	9	1250

Table S 7 Kinetic data from the transient absorption measurements for CAD4|NiO in the presence of I^-/I_3^-. The amplitude weighted average lifetime here is based on τ for comparison with the amplitude weighted lifetime based on logτ provided in the main text.

References

1. A. Dreuw and M. Head-Gordon, *J. Am. Chem. Soc*, 2004, **126**, 4007–4016.

2. T. Yanai, D. P. Tew and N. C. Handy, *Chem. Phys. Lett.*, 2004, **393**, 51–57.